Observation of a Phase Transformation of Ga_2S_3 in a Quartz Effusion Cell above 1230 K by Means of Neutron Scattering

Camille Y. Jones*,† and Jimmie G. Edwards

Department of Chemistry, University of Toledo, Toledo, Ohio 43606

Received: September 16, 2000; In Final Form: December 27, 2000

We report the first neutron scattering study of a condensed-phase transformation in an effusion cell at high temperatures. Neutron powder diffraction patterns of gallium sulfide in a quartz effusion cell were measured from room temperature to 1260 K to seek a phase transformation at 1243 K implied by mass-spectrometric and vapor-pressure data and predicted with a thermodynamic theory of condensed-phase transformations in binary systems. Diffraction patterns in the range of 1230−1260 K revealed a phase transformation from monoclinic Ga_2S_3 to a high-temperature phase, which was indexed from neutron diffraction data at 1260 K as hexagonal with unit cell parameters $a = 3.74 \pm 0.20$ Å and $c = 6.14 \pm 2.69$ Å. Diffuse scattering observed in the diffraction pattern of the hexagonal, high-temperature phase suggested disordering in Ga_2S_3 and correlation in gallium positions on the length scale of their sublattice spacing in the monoclinic phase. The time scale of the experiment, >1 h, prevented a determination of the order of the transformation. This application of time-of-flight neutron powder diffraction to samples in effusion cells has introduced a new high-temperature technique for structural studies of phase equilibria of materials under effusion conditions.

Introduction

The existence of new phases of refractory materials at high temperatures has been determined most often indirectly, by analysis of calorimetric or vaporization data or inspection of sample residues at room temperature, after a heating cycle. Experimental studies of high-temperature phase (HTP) equilibria and thermochemistry of refractories have depended greatly on the techniques of calorimetry, X-ray diffraction, and vaporization measurements. Effusion methods in particular have been used widely for the study of vaporizing systems of refractory materials under conditions of thermodynamic equilibrium at high temperatures. However, for conventional effusion studies such as torsion-effusion or Knudsen-cell mass spectrometry, the stable phases cannot be observed during the experiments. Methods for direct observation of materials inside effusion cells are therefore desired to give clear structural evidence for HTP transformations and to provide a more complete understanding of the relationship between phase transformations and vaporization phenomena. Here we report the use of neutron scattering for direct observations on gallium sulfide, Ga_2S_3, in a fused quartz effusion cell at 298 K < T < 1260 K.[1−3] From the neutron powder diffractograms, we identified a solid−solid-phase transformation which has for more than 20 years been a suspected cause of anomalous vapor pressures above Ga_2S_3 observed during effusion experiments.[4,5]

The monoclinic, low-temperature phase of gallium sulfide, known as α-Ga_2S_3, undergoes the congruent vaporization reaction

$$Ga_2S_3(\alpha) = Ga_2S(g) + S_2(g) \quad (1)$$

where $Ga_2S(g)$ and $S_2(g)$ are the principal species in the vapor.[6] In 1977, Roberts and Searcy[5] reported mass spectrometric data indicating an increase in partial pressure of $Ga_2S(g)$ with a concurrent decrease in $S_2(g)$ partial pressure above gallium sulfide in an effusion cell when the temperature was decreased from 1230 K. They explained this observation on the basis of a transformation between two condensed phases having a slight difference in composition. Since then, similar observations of vapor pressure anomalies have been made during various types of effusion experiments on the Ga−S,[6,7] MnS−Ga_2S_3,[8] and Ga−Se[9,10] systems.

Edwards and Uram[7] explained the anomalous temperature dependence of vapor pressure with multiple equilibrium states. More recently, Edwards and Franzen[11] explained the same phenomenon through a theory of condensed-phase transformations of binary systems in effusion cells. Their theory explains anomalous temperature dependence with a derived thermodynamic relationship among temperature, pressure, and composition during condensed-phase transformations in dynamic vaporization experiments. The theory called for a condensed-phase transformation of Ga_2S_3 at 1240 K, but the HTP was yet to be observed and no corresponding phase transformation appears in any published phase diagrams of the gallium−sulfur system.[12,13] The purpose of the present work was to use time-of-flight neutron powder diffraction to confirm the occurrence of the transformation in an effusion cell, identify the HTP, and confirm the predictions of thermodynamic theory. Whether the HTP was liquid or solid had not been established, but mass-spectrometric data[4] on gallium sulfide were used to assign the congruent vaporization reaction

$$Ga_{2.02}S_3(\text{condensed}) = 1.01Ga_2S(g) + 0.99S_2(g) \quad (2)$$

to the HTP. The melting point of the monoclinic phase of Ga_2S_3 is 1363 K, which is 123 degrees above the temperature of the suspected transformation.

Comparisons of the different structures and phases reported for Ga_2S_3 are difficult to make. For the monoclinic phase, a

* To whom correspondence should be addressed.
† Presently at Metals and Ceramics Division, Oak Ridge National Laboratory, Oak Ridge, TN 37831.

10.1021/jp003312x CCC: $20.00
Published on Web 03/15/2001

clarification of the compound name and a procedure for its synthesis were presented by Uram and Edwards.[14] The monoclinic phase, called α-Ga_2S_3 by Goodyear and Steigmann[15] and α′-Ga_2S_3 by Pardo et al.,[13] has space group *Cc* and unit cell parameters $a = 11.21$ Å, $b = 6.41$ Å, and $c = 7.02$ Å. Collin et al.,[16] Pardo et al.,[13] and Tomas et al.[17] discussed polymorphism in gallium sulfide resulting in the different structures and as a factor causing problems with the reproducibility of direct synthesis of Ga_2S_3. In 1993, Pardo et al.[18] proposed the structure of α-Ga_2S_3 to be monoclinic *Cc* but to comprise three domains with different site occupancies for gallium. In this paper, the low-temperature, monoclinic phase will be called "α-Ga_2S_3" or "LTP", the high-temperature phase will be called "HTP", and "gallium sulfide" or "Ga_2S_3" will be used as a general reference to the material in no specific phase.

Effusion experiments have allowed observations of anomalous temperature dependence of vapor pressure, but the peculiar environment inside the effusion cell has also been shown to facilitate formation of nonstoichiometric compounds and compounds of unusual stoichiometry that could not be synthesized by more conventional methods. While investigating the existence of phases between the compositions YSe and Y_2Se_3, Kim and Franzen[19] discovered the nonstoichiometric compound $Y_{5-x}Se_7$ after heating for 6 h in a tungsten Knudsen cell at 1450 °C. During a vaporization study of the Lu−S system, Kim et al.[20] discovered Lu_3S_4 and a second phase, $Lu_{2+x}S_3$, produced by loss of sulfur from the known compound Lu_2S_3. A new thulium sulfide, $Tm_{15}S_{22}$, was found by Zhang and Franzen[21] in residues from vaporization experiments that also necessarily involved the melting of the sample. The key experimental factor in these investigations was that a molecular-weight effect on effusion rates affected the vapor composition, and thus the chemical equilibrium, inside the cell. For example, because S_2(g) has a mean speed more than 1.5 times that of Ga_2S(g) at a given temperature, the vapor inside the effusion cell is enriched in Ga_2S(g) relative to S_2(g) in order for the two species to pass through the orifice at the same rate. The chemical activities of the species inside the cell are therefore different than those in a closed system or during free vaporization. Because of the unique conditions in the effusion cell, the system can exhibit phase behavior different from that observed during other types of synthesis or heating experiments.[22] It is also of interest to note that among effusion studies, in general, all cases of synthesis of new phases and of anomalous temperature dependence of vapor pressure involve chalcogenides, specifically, sulfides and selenides.

Experimental Section

Sample Preparation. The phase α-Ga_2S_3(s) was prepared from stoichiometric amounts of sulfur (99.999%, Johnson Matthey, Ltd.) and gallium (99.999%, Johnson Matthey, Inc.). The preparation method was the one described elsewhere.[13] The elements were weighed and transferred to a Vycor tube, a small amount of iodine (Alfa Products) was added to aid transport of the reactants, and the tube was evacuated to approximately 2×10^{-3} Torr and sealed with a flame. The sealed tube was heated to 1273 K for 10 days. When the synthesis was complete, the iodine was sublimed to the opposite end of the tube from the product, the tube was opened to ambient conditions, and the product was removed and ground to a fine powder with an agate mortar and pestle. An X-ray diffraction pattern obtained for the starting material matched that of a reference pattern of α-Ga_2S_3.[23]

Direct syntheses and total exhaustion experiments on Ga_2S_3 reported in the literature routinely involved the use of quartz ampules.[14] Physical evidence that there was negligible interaction between Ga_2S_3 and Vycor and quartz container materials used during this work comes from visual inspection under a light microscope of the ampules and effusion cells that were exposed to gallium, sulfur, or Ga_2S_3. None of the containers showed evidence of etching or cracking. In addition, subsequent neutron diffraction studies showed that all of the Bragg scattering could be modeled with the crystal structure of Ga_2S_3. Moreover, no compounds exist containing both Ga and Si together with O and/or S, unless an additional metal such as sodium is present in large proportion. Thus, there is ample evidence of the inertness of quartz and Vycor sample containers used for the synthesis and study of Ga_2S_3.

For the first neutron scattering experiment, experiment 1, the powdered sample was poured into an effusion cell, described in the next section, through a long glass funnel until its height was 1.4 cm. In experiment 2, the effusion cell was filled with sample to a height of 2.2 cm. The height of the sample in the second experiment was increased over that of the sample in the first experiment to ensure that the sample would fill a constant cross section of a neutron beam having nominal dimensions 1.0 cm × 1.27 cm for the entire experiment.

Quartz Effusion Cells. The effusion cells used were designed specifically for these experiments. Two effusion cells, drawn in Figure 1 and called cell A and cell B, were fabricated from commercially available fused quartz tubing in standard sizes with standard taper joints. Cell A, used in experiment 1, was constructed in one piece from quartz tubing having a 10 mm o.d. and 8 mm i.d. Cell B, used in experiment 2, was made from quartz tubing having a 10 mm o.d. and 9 mm i.d. and included a removable, reusable lid with orifice. The thinner walls were intended to decrease the background neutron scattering from the quartz. All other aspects of the design and fabrication of cell A and cell B were the same. To the top of each cell was fused a 1 m quartz tube with a 10 mm o.d. and 8 mm i.d., which allowed the cell to be kept under vacuum. Lids were made from 7/25 standard-taper quartz inner joints. The lid with orifice for cell B is depicted in Figure 2. The orifices for both cells were axial sections of the frustums of right circular cones with length-to-minimum-radius ratios of 4 ± 0.5 and effective orifice areas of 0.15 mm^2.[24] The sizes of the orifices were chosen to allow a convenient rate of mass loss for the time scale of the experiments and ensure that a sufficient amount of sample remained in the neutron beam for the duration of the experiments. For the direction of increasing temperature, the expected transformation time Δt was calculated from the Knudsen equation:

$$P_K = (\Delta g/\Delta t)(2\pi RT/M_{avg})^{1/2}(1/A_{eff}) \quad (3)$$

where P_K is the vapor pressure inside the cell, Δg is the loss of mass of sample required to change the composition of 1 g of α-Ga_2S_3 to that of the HTP $Ga_{2.02}S_{2.98}$,[4] when only S_2 is assumed to be in the vapor, R is the gas constant, T is the temperature in Kelvins, and M_{avg} is 0.064 kg mol^{-1}. For this work, Δt was 3.9×10^3 s with the variables $P_K = 7.38$ Pa, $\Delta g = 4.074 \times 10^{-6}$ kg, $T = 1240$ K, and $A_{eff} = 1.43 \times 10^{-8}$ m^2.

Instrument Configuration. Experiments were performed at the Glasses, Liquids, and Amorphous Solids diffractometer (GLAD)[25] at the Intense Pulsed Neutron Source at Argonne National Laboratory. Figure 3 shows a schematic representation of the apparatus, which was set up at the downstream sample well at the GLAD. Table 1 lists the dimensions of the major components of the apparatus in the path of the beam. A vanadium-foil furnace under vacuum was used to heat the

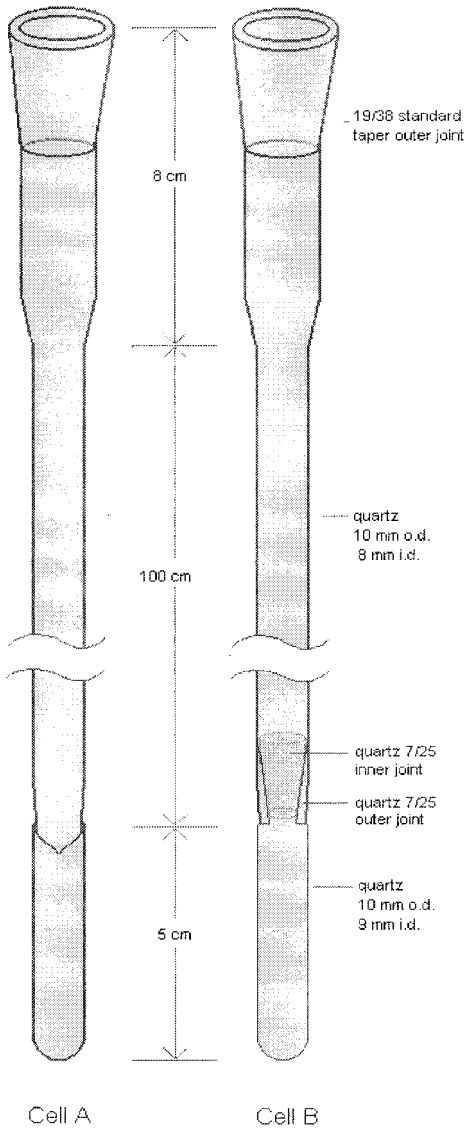

Figure 1. Designs and dimensions of the effusion cells.

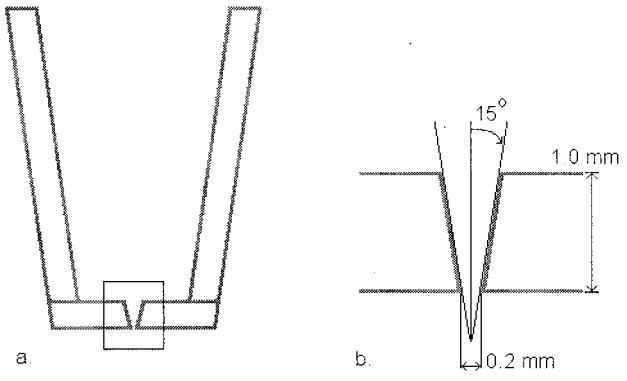

Figure 2. Dimensions of the orifice of cell B.

effusion cell and sample, which were in a separate vacuum system. A standard taper joint at the top of the condensation tube was connected to the inlet of a liquid nitrogen trap, which was connected to a vacuum system by flexible stainless steel tubing. The cell and trap were evacuated to 10^{-5} Torr. The temperature of the sample was determined by a type-K thermocouple placed directly underneath a pedestal on which the effusion cell was resting. During measurements of the temperature of the empty furnace, the temperature difference between

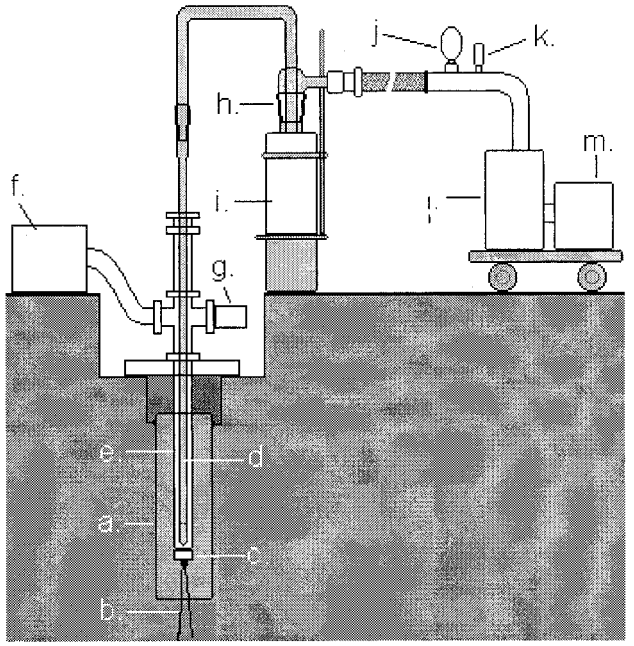

Figure 3. Schematic of experiment setup: a. furnace and radiation shields; b. thermocouple; c. sample pedestal; d. effusion cell; e. sample well; f. turbo pump; g. pressure gauge; h. trap; i. dewar filled with liquid nitrogen; j. ion gauge; k. thermocouple pressure gauge; l. oil diffusion pump; m. mechanical pump. The shaded area is a large evacuated chamber for the flight path.

TABLE 1: Dimensions of Instrument Components in the Path of the Neutron Beam

component	actual height (cm)	height used for calculations (cm)	inner radius (cm)	outer radius (cm)
Ga_2S_3				
before experiment	1.4	1.1	0.00	0.4
Ga_2S_3				
after experiment	0.8	1.1	0.00	0.4
effusion cell	5	6.00	0.4	0.5
Howe furnace:				
element			2.5973	2.61
inner heat shield		9.3873	9.4	
outer heat shield		9.8873	10.0	

the sample position and the position of the control thermocouple was observed to increase linearly with the temperature setting by 2° cm^{-1} across the location of sample. A correction factor was applied to each temperature setting to obtain the desired temperature at the sample position.

Data Collection and Analysis. In experiment 1, neutron diffraction data were collected in 13 runs. Five runs were performed in the absence of a sample for the purposes of determining a background correction and for normalization: 1. vanadium standard; 2. empty sample well; 3. empty furnace; and 4. and 5. furnace and empty effusion cell at two temperatures. Eight runs with a sample were performed at several different temperatures: 6. increase from room temperature to 773 K over 40 min; 7. increase temperature from 773 to 1173 K over 40 min; 8. at 1230 K for 4 h; 9. at 1230 K for 8 h; 10. at 1260 K for 4 h; 11. at 1260 K for 8 h, 12. at 1200 K for 5 h; 13. at 1200 K for 8 h. Sample runs 8, 10, and 12 were performed to allow time for the sample to transform before the 8 h data sets 9, 11, and 13 were collected. The temperature was increased to a new set point at a rate of 5° min^{-1} or decreased by natural cooling to a new set point.

In experiment 2, neutron diffraction data were collected in eighteen runs: 1. vanadium standard; 2. and 3. empty cell at

room temperature for 1 h; 4. empty effusion cell at 1200 K; and 5. empty effusion cell at 1260 K. Thirteen runs were performed with at the following for a sample: 6. for 1 h while establishing a vacuum; 7. at 1230 K for 1 h; 8. at 1230 K for 8 h; 9. at 1230 K for 1 h; 10. at 1260 K for 4 h; 11. at 1260 K for 1 h; 12. at 1260 K for 8 h; 13. at 1260 K for 1 h; 14. at 1170 K for 6 h; 15. at 1170 K for 1 h; 16. at 1170 K for 8 h; 17. at 1170 K for 1 h; and 18. empty furnace at room temperature. Runs 2 and 3 were performed to determine the change in scattering intensity when the cell was removed from the beam between successive runs. To see this effect, the cell was placed in the furnace and data were collected for 1 h at room temperature, then it was completely removed from the furnace, and the entire procedure was repeated. The cell was marked so it could be placed into the furnace in the same orientation each time. The data were normalized according to standard procedure[26,27] and the results were compared both visually and quantitatively for differences outside the statistical precision of the measurement. In addition, six 1-h runs, the odd-numbered runs 7−17, were performed periodically to allow estimation of the change in total scattered neutron intensity from the sample with time.

The data were analyzed by an established procedure.[27] The increment and maximum values of momentum transfer $\boldsymbol{Q}$ were 0.015 and 40 Å^{-1}, respectively. The neutron counts included in the analysis were those detected in the ranges $8° < 2\theta < 125°$, where 2θ is the scattering angle, and $0.1 < \lambda < 8.0$ Å, where λ is the wavelength. Raw neutron counts were corrected for detector efficiency and dead time, delayed neutron fraction, and then normalized to the incident beam monitor spectrum. Intensity corrections were applied to the vanadium standard data, which were then smoothed. Numerical corrections for absorption and multiple scattering from cylindrical geometries were performed for the furnace, furnace shields, effusion cell, and sample.

Results

Neutron Diffraction Patterns. The height of the sample in experiment 1 decreased below the nominal height of the neutron beam, and the 1 mm thick cell walls gave high intensity of amorphous scattering from quartz. In experiment 2, the larger sample kept the sample height above the nominal height of the neutron beam and the thinner cell walls gave lower amorphous background under the scattering from the sample. We present only the results of experiment 2 for further discussion. The total neutron count from each of six odd-numbered runs 7−17 was divided by the number of time-of-flight pulses received by the sample during each corresponding 1 h period, and the resulting ratios were plotted against time. This plot, shown in Figure 4, is nearly linear and has a negative slope that yields an estimated decrease in total neutron count of 0.04% per hour. This rate is comparable to the rate of effusion calculated from eq 3; therefore, the decrease in total neutron count can be attributed to a decrease in the mass of the sample. The decrease in the total neutron count at a given angle of detection during one run was generally of similar or greater magnitude than the intensity corrections for absorption and multiple scattering.

Plots of diffraction patterns are shown for the data at 1230, 1260, and 1170 K in Figure 5. The diffraction patterns taken at 1230 and 1170 K matched the room-temperature X-ray diffraction pattern of the starting material, summarized in Table 2, after adjustment for thermal expansion and differences in resolution and relative intensities between the two methods. When the temperature of the sample was raised from 1230 to

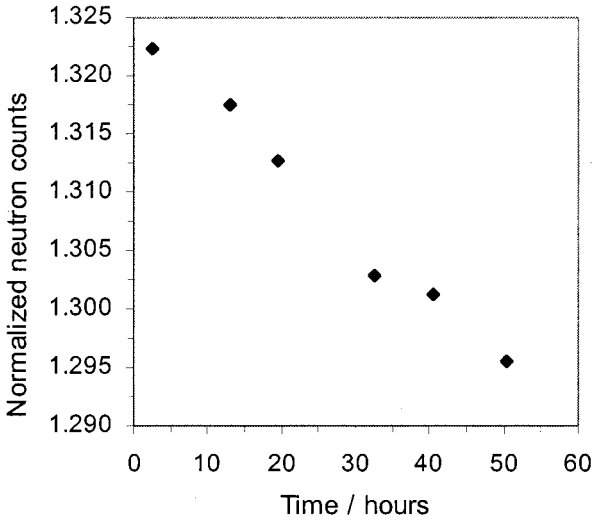

Figure 4. Normalized neutron counts vs time of sample in neutron beam. The normalized neutron counts were calculated from the ratio of total counted neutrons to total incident neutrons.

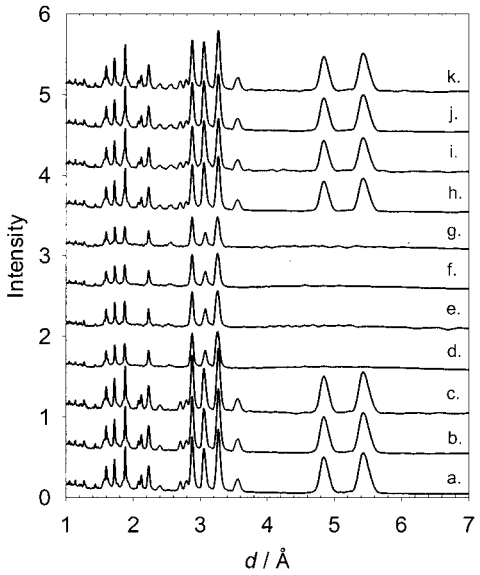

Figure 5. Neutron powder diffractograms from experiment 2, taken at several temperatures: a. 1230 K, 1 h; b. 1230 K, 8 h; c. 1230 K, 1 h; d. 1260 K, 4 h; e. 1260 K, 1 h; f. 1260 K, 8 h; g. 1260 K, 1 h; h. 1200 K, 4 h; i. 1170 K, 1 h; j. 1170 K, 8 h; k. 1170 K, 1 h. Each plot is offset by 0.5 units on the intensity axis relative to the previous plot. Data were collected in the order a−k.

1260 K, two major Bragg peaks vanished, with some small changes in the relative spacings of the others, and some of the minor reflections disappeared. When the temperature of the sample was reduced from 1260 to 1170 K, the Bragg peaks that had disappeared then reappeared but were less intense and had different relative intensities. Diffuse scattering from the HTP was observed in the diffraction pattern at 1260 K in the range $0.5 < \boldsymbol{Q} < 3$ Å^{-1}, as shown in the overlay plot in Figure 6. In the powder pattern of α-Ga_2S_3, this is the location of three large Bragg reflections, the *110* reflection at $\boldsymbol{Q} = 1.17$ Å^{-1} and the unresolved reflections *200* and *111* at $\boldsymbol{Q} = 1.3$ Å^{-1}.

The eighteen most intense reflections from the diffraction pattern of the HTP were indexed as hexagonal. The results of the indexing are listed in Table 3. The unit cell parameters and least-squares estimates of their standard error are $a = 3.74$ (0.20) Å and $c = 6.14$(2.69) Å. The large uncertainties and predominantly negative residuals were a result of estimating d-

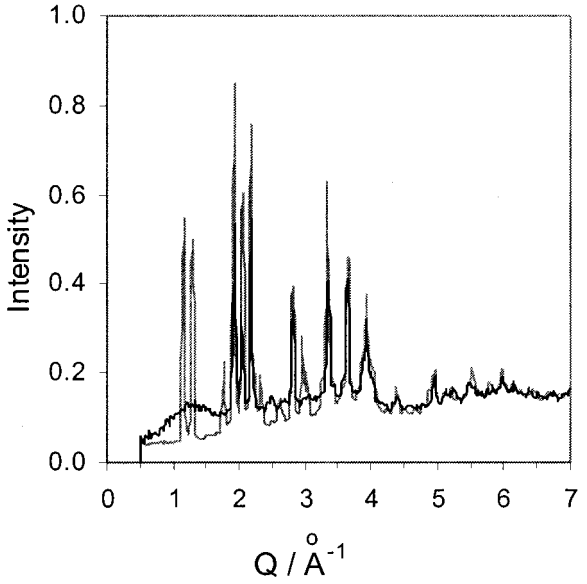

Figure 6. Overlay of diffractograms from Figure 5 parts a (grey line, 1230 °C) and f (black line, 1260 °C), that shows the increase in diffuse scattering at low ***Q*** in the data collected at 1260 K.

TABLE 2: Powder Diffraction Data on the Monoclinic Phase of Ga_2S_3

	X-ray diffraction starting material at room temperature		neutron diffraction low-temperature phase at 1230 K		
hkl	*d*/Å	I/I_0	***Q***/Å^{-1}	*d*/Å	I/I_0
110	5.311	22	1.150	5.464	23
200	4.753	32	1.300	4.833	19
111	3.500	5	1.775	3.540	9
−311, 020	3.206	48	1.925	3.264	32
−112, 002	3.007	100	2.050	3.065	28
021, −312	2.820	80	2.175	2.889	32
−221	2.741	5	2.250	2.793	9
220	2.655	8	2.325	2.702	8
112	2.342	18	2.625	2.394	6
221, 311	2.205	54	2.825	2.224	12
202	2.098	9	2.950	2.130	9
−511			3.025	2.077	6
−602, −331	1.850	61	3.325	1.890	15
−404	1.707	30	3.650	1.721	12
−514	1.585	6	3.850	1.632	5
−622, 040	1.579	63	3.925	1.601	9
331			4.000	1.571	5
−333, −114			4.250	1.478	3

spacing *d* from the apexes of the reflections, which were broad and asymmetric. A Rietveld analysis of high-resolution time-of-flight neutron powder diffraction data on the HTP[28] yielded more accurate lattice parameters, $a = 3.73053(6)$ Å and $c = 6.0961(2)$ Å, and uncertainties distributed about zero.

Figure 7 shows a graphical representation of the relationship between the monoclinic (m) and hexagonal (h) unit cells of the LTP and HTP. A transformation matrix $\boldsymbol{T}_h$ exists[29] and yields the linear transformations

$$\boldsymbol{a}_h = 1/3(\boldsymbol{a}_m) \tag{4a}$$

$$\boldsymbol{b}_h = -1/5(\boldsymbol{a}_m) + 1/2(\boldsymbol{b}_m) \tag{4b}$$

$$\boldsymbol{c}_h = 1/3(\boldsymbol{a}_m) + \boldsymbol{c}_m \tag{4c}$$

The metric tensor $\mathbf{G}_h$ for the hexagonal unit cell is given by

$$\mathbf{G}_h = \boldsymbol{T}_h^{\,T}\, \mathbf{G}_m\, \boldsymbol{T}_h \tag{5}$$

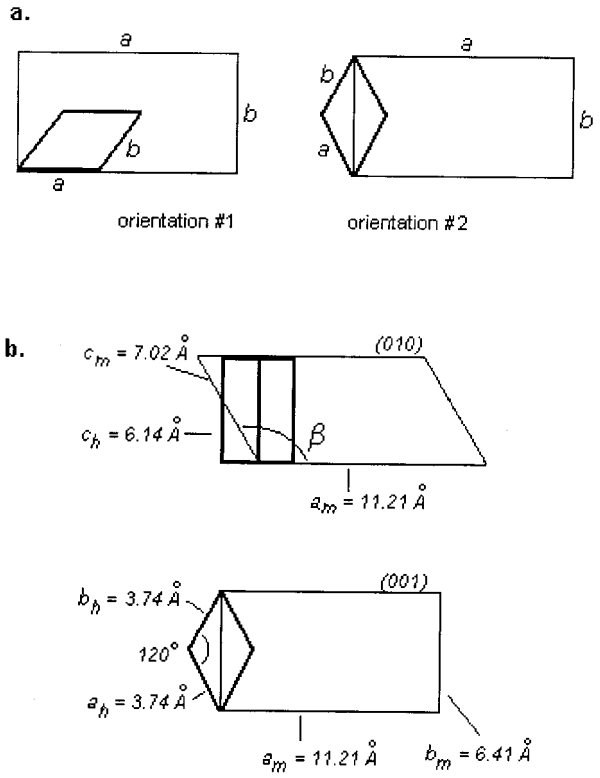

Figure 7. (a) Two unique relative orientations of the monoclinic and hexagonal unit cells of gallium sulfide. Orientation 2 was used for calculation of the transformation matrix. (b) Projections of the monoclinic and hexagonal unit cells with relative orientation 2. The angles between the direct-space basis vectors of the hexagonal cell and the reciprocal-space vectors of the monoclinic cell, measured about a common origin *O* are as follows: $\angle a_hOa^*_m$, 66°; $\angle a_hOb^*_m$, 148.83°; $\angle a_hOc^*_m$, 90°; $\angle b_hOa^*_m$, 66°; $\angle b_hOb^*_m$, 30°; $\angle b_hOc^*_m$, 90°; $\angle c_hOa^*_m$, 58.83°; $\angle c_hOb^*_m$, 90°; $\angle c_hOc^*_m$, 0°.

TABLE 3: Indexing Results on the HTP of Ga_2S_3 at 1260

[*hkl*]	*d*(obs)/Å	*d*(calc)/Å	*d*(obs) − *d*(calc)/Å
205	0.9733	0.999	−0.026
302	1.0158	1.029	−0.013
213	1.0464	1.065	−0.018
300	1.0773	1.088	−0.011
212	1.1406	1.149	−0.009
114	1.1965	1.211	−0.014
203	1.2645	1.29	−0.026
202	1.4634	1.45	0.013
201	1.5614	1.581	−0.019
112	1.5906	1.619	−0.028
200	1.6150	1.632	−0.017
103	1.7197	1.77	−0.05
110	1.8646	1.885	−0.02
102	2.2161	2.271	−0.055
101	2.8535	2.901	−0.047
002	3.0460	3.16	−0.114
100	3.2293	3.265	−0.036
lattice parameters:	$a = 3.74$ (0.20) Å $c = 6.14$ (2.69) Å		

and shows rough agreement with that calculated from

$$\mathbf{G}_h = \mathbf{A}_h^{\,T}\, \mathbf{A}_h \tag{6}$$

where $\mathbf{A}_h$ is a 1×3 row vector of the hexagonal basis vectors from the aforementioned Rietveld refinement. Hexagonal basis vectors back-calculated from eq 4 are $\boldsymbol{a}_h = 3.690$ Å, $\boldsymbol{b}_h = 3.719$ Å, and $\boldsymbol{c}_h = 6.090$ Å. The matrix $\boldsymbol{T}_h$ has a determinant of 0.167, a positive nonzero value; therefore, the basis vectors $\boldsymbol{T}_h$ yields are independent and describe a right-handed coordinate system.[30]

Mass Loss and Sample Residues. In this section, primarily results from experiment 1 are presented. The color and appearance of the residue from experiment 1 were similar to those of the starting sample, except the height of the sample had diminished by ~25%. Small amounts of several different colors of crystallites—yellow, brown, and amber—were present at the surface of the residue; yellow and pale yellow crystals were present underneath the surface of the residue as well as around the orifice in the top of the cell. Powder patterns of several samples of the residue were taken, values of *d* were calculated for the lines, and the line intensities were estimated visually and assigned a numerical value from 1 to 20. The diffraction pattern of the pale yellow residue matched that of the starting material. The pattern for the yellow residue contained predominantly lines characteristic of GaS. The diffraction pattern of the brown residue did not match the pattern of the starting material, nor did it match any published diffraction patterns for compounds in the Ga−S, Ga−O, or Ga−O−S systems. Attempts to index the d spacings of the brown residue as cubic, on the basis of the simplicity of the diffraction pattern, were not successful. However, the general appearance of the pattern was that of the diamond-cubic structure.

A single crystal was selected from the pale yellow residue in the upper interior part of the cell and analyzed by single-crystal X-ray diffraction. The resulting single-crystal structure was the same as that of α-Ga_2S_3 determined by Goodyear and Steigmann.[15]

Outside of the effusion cell, white and yellow bands of residue had deposited in the condensation tube. The powder pattern of the white material matched that of α-Ga_2S_3, and the powder pattern of the yellow material matched that of GaS. An orange residue, believed to be amorphous sulfur, coated the inlet of the liquid nitrogen trap and the inner tube immediately after the experiment. With time in air, the orange residue lost some of the intensity of its color.

After experiment 2, the residue of Ga_2S_3 in the effusion cell was the same color as the starting material. Bands of colored residues appeared outside the cell as in experiment 1. The sample had undergone coarsening, and the height of the sample had diminished by ~25%.

Discussion

HTP of Ga_2S_3. This work has demonstrated the condensed-phase transformation in Ga_2S_3 at 1240 K proposed by Roberts and Searcy[5] and later called for by the theory of Edwards and Franzen.[11] For the first time, condensed phases in an effusion cell were observed directly at high temperatures. However, on the time scale of this experiment, confirmation of the three-phase equilibrium was not obtained.

That previous reports of hexagonal phases of Ga_2S_3 represent the same phase as reported here is uncertain. In 1949, Hahn and K1ingler[31] reported a hexagonal phase called β-Ga_2S_3, with $a = 3.678$ Å and $c = 6.016$ Å. Six years later, Hahn and Franck[32] reported a hexagonal phase called α-Ga_2S_3, with $a = 6.383$ Å and $c = 18.04$ Å, and assigned it the possible space groups $P6_1$ or $P6_5$. Pardo et al.[17] reported a hexagonal phase called β-Ga_2S_3 and proposed a wurtzite-type structure. A hexagonal phase was not found in residues from effusion experiments inspected at room temperature.

A comparison of the structures of α-Ga_2S_3 and wurtzite was previously made by Goodyear and Steigmann.[15] They described the crystal structure of α-Ga_2S_3 as having sulfur atoms in a "nearly hexagonally close-packed" (hcp) arrangement in layers perpendicular to $[\bar{1}01]$ and with gallium atoms occupying two-thirds of the tetrahedral sites occupied by zinc atoms in wurtzite. They calculated S−S distances around the vacant tetrahedral sites, found they were shorter than S−S distances surrounding tetrahedral interstices occupied by gallium atoms, and suggested that this "shrinkage" of the tetrahedra of sulfur atoms around the ordered vacancies distorted the hcp arrangement of the sulfur atoms. The description of the structure of α-Ga_2S_3 given by Goodyear and Steigmann, along with the general appearance and hexagonal indexing of the neutron powder diffraction pattern for the HTP, suggests that disordering in Ga_2S_3 might be occurring among the gallium and vacancy sites. If the Ga_2S_3 structure were distorted from hexagonal symmetry because of shorter S−S bond lengths around vacant sites, then occupation of vacant sites by gallium atoms through the disordering process could increase the S−S bond lengths and remove distortion. At the same time, the sulfur atoms in the HTP could assume an hcp arrangement, and accordingly, the sulfur sublattice, no longer distorted, would take on a hexagonal symmetry.

To test the hypothesis that disordering of gallium atoms and vacancies occurred during the transition of α-Ga_2S_3 to the HTP, structure factors were calculated for the monoclinic structure model for α-Ga_2S_3 and for a wurtzite-type model for the HTP. Calculations for the individual sulfur and gallium sublattices of the monoclinic structure show that the *110*, *200*, and *111* reflections originate from a sublattice of gallium atoms. Structure factors calculated for a hypothetical α-Ga_2S_3 structure with all ordered vacancies occupied by gallium yielded *110*, *200*, and *111* reflections that were weak but still present. Structure factors for a wurtzite-type structure with the unit cell parameters of the HTP and atom positions taken from wurtzite showed no reflections in the vicinity of the *110*, *200*, and *111* reflections of the monoclinic model. Because no reflections appear in the neutron powder diffractograms of the HTP in the vicinity of the *110*, *200*, and *111* reflections, the hexagonal model was chosen for the HTP. The structure factors clearly suggest that disordering of Ga_2S_3 involves only the sites of gallium and vacancies in the original monoclinic phase. In addition, the maximum in the diffuse scattering, which roughly coincides with the *110*, *200*, and *111* reflections, suggests that the Ga atoms, although disordered, possess short-range order on a length scale similar to the distance between their lattice sites in α-Ga_2S_3.

A characterization of the observed phase transformation as either continuous or discontinuous is not possible on the time scale of the present experiment. The usual characteristics in the diffraction patterns of materials undergoing order−disorder transformations are a gradual disappearance of superlattice lines with increasing temperature and an acceleration of the disappearance of the superlattice lines near the transformation temperature. Crystallographically, the space group of the low-symmetry form, LTP, must be a subgroup of the space group of the high-symmetry form, HTP. The point group of the LTP, *m*, is a subgroup of 6*mm*, the point group for the HTP. Although group−subgroup relationships are not sufficiently restrictive to be useful,[33] the existence of this relation allows the possibility of an order−disorder transformation showing continuity on a time scale shorter than that of the present experiment. Also, while it is true that the LTP and HTP have slightly different compositions, the time scale of the structural change relative to that of the composition change has not yet been established.

Thermodynamic Aspects of the Phase Transformation. Under the present experimental conditions, there was no evidence for either a mixture of two solid phases, as would occur in a three-phase equilibrium, or a gradual change in the structure, as would be expected for an order−disorder transformation. To

observe a three-phase equilibrium with gradual appearance and disappearance of the HTP and LTP, respectively, each successive diffraction pattern would have to be measured in minutes on an instrument giving high resolution of Bragg peaks. In the present study, data were collected for one to several hours in order to achieve sufficient intensity.

Data from vaporization experiments have provided a value for the standard molar enthalpy of vaporization $\Delta_v H°$ for the LTP[14] and theory has provided estimates of $\Delta_v H°$ for the HTP.[11] From these, a standard molar enthalpy of transformation $\Delta_{tr} H°$ for the reaction HTP(s) = LTP(s) was estimated.[11] Because plots of ln P versus $1/T$[14] showed no change in slope at 1220−1240 K, a small value for $\Delta_{tr} H°$ is implied. Although values for $\Delta_{tr} H°$ for disordering transformations vary with the types of structures and bonds involved, a value of $\Delta_{tr} H°$ for a transformation involving disordering of gallium and vacancies with no change in the coordination of Ga or S is expected to be much smaller than the heat of fusion. The present structural evidence for disordering of Ga in Ga_2S_3 is therefore consistent with theory,[11] for which values for $\Delta_{tr} H°$ of less than 10 kJ mol^{-1} are required to reproduce the shape of the three-phase curve and the temperature of the onset of a transformation that passes through a three-phase equilibrium.

The HTP must be slightly rich in Ga relative to the LTP to reproduce the observed vapor pressure anomalies, vapor composition changes, and transformation temperature with theory. The increase in gallium concentration in Ga_2S_3 corresponds to an increase in configurational entropy $\Delta S°_{config}$ over that occurring with no change in composition. The gain in $\Delta S°_{config}$ expected for the HTP with no change in composition, with two gallium atoms and one vacancy occupying three tetrahedral sites, is R ln(3/2) = 3.37 J mol^{-1} K^{-1}. For the entropy of transformation $\Delta_{tr} S°$, Edwards and Franzen used 6.5416 J mol^{-1} K^{-1}, which corresponded to their lowest estimate of $\Delta_{tr} H°$ for the transformation, 8 kJ. Their value of $\Delta_{tr} S°$ is greater than $\Delta S°_{config}$ by 3.08 J mol^{-1} K^{-1}.

Conclusions

This work has demonstrated the condensed-phase transformation in Ga_2S_3 at 1240 K proposed by Roberts and Searcy and later called for by the theory of Edwards and Franzen. For the first time, condensed phases in an effusion cell were observed directly at high temperatures. The structure factors show that disordering of Ga_2S_3 involves only the sites of gallium and vacancies in the original monoclinic phase.

Neutron diffraction study of the binary system Ga−S in effusion cells has provided a complementary technique to vaporization for the study of the anomalous vapor-pressure effects in Ga_2S_3. The study of other systems known to exhibit similar anomalous changes in vapor pressures may lead to a general understanding of phase equilibria and their temperature dependence. Further progress in this area would be aided by the use of furnaces with longer isothermal regions to ensure that the entire effusion cell is at the same temperature. The time dependence of these phenomena may be revealed by collection of data on time scales on the order of seconds or minutes during the phase transformation.

Acknowledgment. This research was sponsored by the U.S. Department of Energy, Office of Science, Office of Basic Energy Sciences, Division of Materials Sciences, under Contract W-31-109-ENG-38 with the University of Chicago. The authors thank Kenneth Volin, Steve Moder, Jackie Johnson, Bryan Chakoumakos, Fritz Franzen, and Yaspal Badyal for their assistance with this work.

References and Notes

(1) Jones, C. Y. Ph.D. Dissertation, University of Toledo, May 1999.
(2) Jones, C. Y.; Edwards, J. G. Neutron Diffraction of Condensed Phases inside Effusion Cells. In *Proceedings of the Materials Research using Cold Neutrons at Pulsed Neutron Sources Conference*; Loong, C.-W., Ed.; World Scientific: London, 1999.
(3) Jones, C. Y.; Edwards, J. G. Neutron Diffraction Studies of Phase Transitions under Effusion Conditions. In *Proceedings of the Tenth International Conference on High-Temperature Materials Chemistry*; Hilpert, K., Ed., April 2000, submitted.
(4) Kashkooli, I. Y.; Munir, Z. A. *High Temp. Sci.* **1972**, *4*, 82.
(5) Roberts, J. A.; Searcy, A. W. *Science* **1977**, *196*, 525.
(6) Starzynski, J. A.; Edwards, J. G. *High Temp. Sci.* **1981**, *14*, 63.
(7) Edwards, J. G.; Uram, R. S. *J. Phys. Chem.* **1992**, *96*, 8561.
(8) Gates, A. S.; Edwards, J. G. *J. Phys. Chem.* **1980**, *84*, 3263.
(9) Dieleman, J.; Sanders, F. H. M.; van Dommeln, J. H. J. *Philips J. Res.* **1982**, *37*, 204.
(10) Viswanathan, R.; Edwards, J. G. *J. Phys. Chem. B* **1998**, *102*, 2419.
(11) Edwards, J. G.; Franzen, H. F. *J. Phys. Chem.* **1995**, *99*, 4779.
(12) Lieth, R. M. A.; Heijligers, H. J. M.; v. d. Heijden, C. W. M. *J. Electrochem. Soc.* **1966**, *113*, 798.
(13) Pardo, M. P.; Tomas, A.; Guittard, M. *Mater. Res. Bull.* **1987**, *22*, 1677.
(14) Uram, R.; Edwards, J. G. *Thermochim. Acta* **1992**, *204*, 221.
(15) Goodyear, J.; Steigmann, G. A. *Acta Crystallogr.* **1963**, *16*, 946.
(16) Collin, G.; Flahaut, J.; Guittard, M.; Loireau-Lozach, A.-M. *Mater. Res. Bull.* **1976**, *11*, 285.
(17) Tomas, A.; Pardo, M. P.; Guittard, M.; Guymont, M.; Famery, R. *Mater. Res. Bull.* **1987**, *22*, 1549.
(18) Pardo, M. P.; Guittard, M.; Chilouet, A.; Tomas, A. *J. Solid State Commun.* **1993**, *102*, 423.
(19) Kim, S.-J.; Franzen, H. F. *J. Less-Common Met.* **1988**, *138*, L29−L32.
(20) Kim, S.-J.; Anderegg, J. W.; Franzen, H. F. *J. Less-Common Met.* **1990**, *157*, 133.
(21) Zhang, Y.; Franzen, H. F. *J. Less-Common Met.* **1991**, *168*, 377.
(22) Edwards, J. G.; Burckel, P. M.; Norwisz, J. *Thermochim. Acta* **1999**, *340−341*, 323.
(23) *Powder Diffraction File*, JCPDS-ICDD, 1985, Card No. 16-500.
(24) Edwards, J. G.; Freeman, R. D. *High Temp. Sci.* **1980**, *12*, 197. Effective orifice area is the actual orifice area multiplied by the transmission probability, which depends on the shape of the orifice.
(25) Ellison, A. J. G.; Crawford, R. K.; Montague, D. G.; Volin, K. J.; Price, D. L. *J. Neutron Res.* **1993**, *1* (4), 61.
(26) Soper, A. K.; Howells, W. S.; Hannon, A. C. *Rutherford Appleton Laboratory Report RAL-89-046*, 1989.
(27) Ellison, A. J. G. *GLAD: A User's Manual*, version 1.1, May 30, 1995.
(28) Jones, C. Y.; Edwards, J. G. Unpublished results.
(29) Boisen, M. B.; Gibbs, G. V. *Mathematical Crystallography*; Mineral Society of America: Washington, DC, 1990; p 71.
(30) *International Tables for Crystallography*, Volume A; p 70 ff.
(31) Hahn, V. H.; Klingler, W. *Z. Anorg. Allg. Chem.* **1949**, *259*, 135.
(32) Hahn, V. H.; Franck, G. *Z. Anorg. Allg. Chem.* **1955**, *278*, 333.
(33) Franzen, H. F. *Chem. Mater.* **1990**, *2* (5), 486.